1.681-eV luminescence center in chemical-vapor-deposited homoepitaxial diamond films

H. Sternschulte, K. Thonke, and R. Sauer
Abteilung Halbleiterphysik, Universität Ulm, D-89069 Ulm, Germany

P. C. Münzinger
Abteilung Festkörperphysik, Universität Ulm, D-89069 Ulm, Germany

P. Michler
4. Physikalisches Institut, Universität Stuttgart, D-70550 Stuttgart, Germany
(Received 28 March 1994)

The 1.681-eV luminescence center characteristically observed in chemical-vapor-deposited diamond films is studied in a homoepitaxially grown diamond film. Homoepitaxial growth relaxes the strain typical for films grown on heterosubstrates with lattice mismatch, thus reducing dramatically the optical linewidths down to 0.2 meV. The no-phonon luminescence transition that we observe exhibits fine structure consisting of a fully resolved doublet with line components at 1.6820 and 1.6828 eV. The doublet thermalizes with an activation energy of (0.80 ± 0.04) meV equal to the spectroscopic spacing of 0.8 meV. In addition, either doublet component has itself an associated close satellite in a mirrorlike arrangement. Three other partly resolved lines enhance the total number of components in the no-phonon transition to at least seven. Photoluminescence and photoluminescence excitation measurements under uniaxial stress along the $\langle 001 \rangle$ crystal direction reveal a splitting of the no-phonon structure into four main components. These are studied at varying temperatures and stress values for their thermalization behavior. We deduce an electronic level scheme of two excited states from which electrons radiatively relax to two lower states. The data are not consistent with excitonic recombination or electron-to-hole recombination. They indicate that the optical center is under uniaxial internal overpressure of approximately 0.06 GPa, probably due to its large size. The luminescence decay time of the optical center was measured to be 4 ns (5 K) through 2.7 ns (300 K) in the homoepitaxial film and $\approx$1 ns nearly independent of temperature in a polycrystalline diamond film.

INTRODUCTION

Optical studies of synthetic diamond films grown on various heterosubstrates by chemical-vapor-deposition (CVD) techniques have revealed the production of a luminescence center with emission energy at 1.681 eV. The center was first observed in 1981 by Vavilov *et al.*[1] in cathodoluminescence (CL) investigations of CVD homoepitaxial diamond layers and polycrystalline diamond heterofilms. Since then, it has been reported in films grown by a variety of CVD methods including hot-filament,[2–4] dc-plasma,[5] microwave-plasma,[6–8] and oxygen-acetylene combustion.[3] This very universal appearance demonstrates the center to be characteristic of CVD diamond.

The origin of the center is not yet clear. However, arguments were advanced that the center contains silicon and, in addition, nitrogen. Zaitsev *et al.*[9] observed the CL spectrum in natural diamond after silicon implantation, and from a quadratic dependence of the CL intensity on the implantation dose deduced the incorporation of two silicon atoms. Collins *et al.*[7] also implanted diamond with ^{29}Si atoms and cofirmed that silicon is involved in the production of the center. Yokota *et al.*[6] found that in their CVD diamond the intensity of the defect luminescence depended on the nitrogen concentration. This was corroborated by the data of Collins *et al.*[7] who observed that the defect spectrum was much stronger after ^{29}Si implantation in synthetic diamond with a high concentration of isolated nitrogen atoms than with a low nitrogen concentration. The spectrum was not detectable in implanted natural semiconducting diamond with negligible nitrogen concentration. Very recently, Collins *et al.*[10] have argued that the optical center involves a vacancy trapped at another defect which is associated with silicon. This conclusion was derived from the observation that the 1.681-eV defect line increased when the photoluminescence (PL) line of the *GR*1 defect (the isolated neutral vacancy) annealed out. The latter work also reports a doublet splitting of the 1.681-eV line. The two components thermalize with their spectroscopic spacing of 0.8 meV. The observation of the doublet structure in Ref. 10 was made possible by the relatively small linewidth, of order 0.8 meV, in the free-standing plates of polycrystalline CVD diamond used, whereas previously reported spectra exhibit linewidths from 3 meV (Ref. 7) up to 10 meV or more.[3,8,11,12]

In the present paper, we study the defect PL spec-

0163-1829/94/50(19)/14554(7)/$06.00

trum in a homoepitaxially grown diamond film in which the linewidths are dramatically reduced. The film was deposited on a (100)-oriented Sumitomo type Ib diamond single crystal in a microwave-plasma-assisted CVD apparatus. The CH_4/H_2 plasma was generated by a magnetron operating at 2.45 GHz. The CH_4 concentration was 3.5% and the growth temperature was 800 °C. Within two hours, a 0.54 μm thick monocrystalline film was grown as proved by studies. As the substrate was located on a stainless-steel substrate holder in a fused-silica chamber it is very natural to assume that Si from the silica was transferred in trace amounts to the substrate to form the optical center. Also, nitrogen is a probable contaminant in the gases used. In the PL measurements the sample was mounted in a continous-flow liquid helium cryostat allowing for temperature control from 2 K to 270 K. The PL was excited by the 488-nm line of an argon ion laser or, in the photoluminescence excitation (PLE) measurements, by a tunable titanium-sapphire laser. The PL signal was dispersed by a 1 m monochromator, detected by a R636-photomultiplier tube, and processed using conventional lock-in techniques. The decay time measurements were performed with excitation by 5-ps pulses from a synchronously pumped mode-locked cavity-dumped Rhodamine 6G dye laser. The optical signal was detected by a photomultiplier and analyzed by a time correlated single photon counting technique providing a time resolution of the order 150 ps.

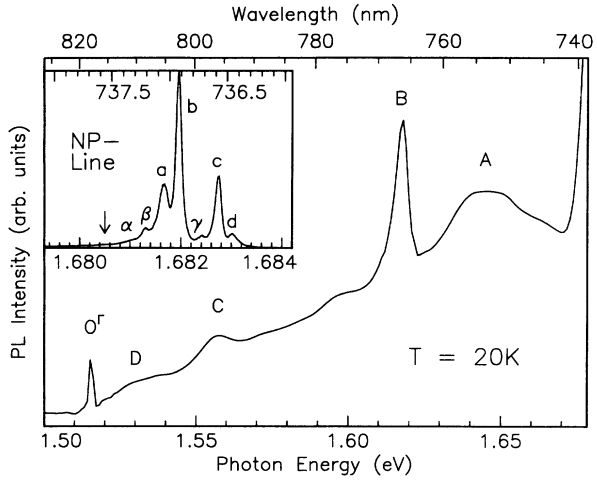

FIG. 1. Low temperature (20-K) PL spectrum of the 1.681-eV defect. The vibronic sidebands are discussed in the text. Notation A–D is according to Ref. 11. Satellite B corresponds to a defect local mode (64.6 meV), and the narrow satellite at 1.516 eV to the O^Γ lattice mode. Inset: Spectral structure of the no-phonon transition at 20 K exhibiting well resolved fine structure (see text).

I. HIGH-RESOLUTION SPECTRUM

Figure 1 shows a survey PL spectrum of the 1.681-eV defect. The no-phonon (NP) transition at 1.682 eV is accompanied by a structured vibronic sideband. Observed are broad satellite lines at energy spacings from the NP line of $\hbar\Omega$ = 42 meV (A), 85 meV, 125 meV (C), and 153 meV (D). Relatively sharp vibronic features arise at displacement energies of 64.6 meV (B) and 166 meV. The vibronic energies are compared in Table I with literature data. The modes A through D were already observed by Feng and Schwartz[11] in their study of the 1.681-eV line in microwave plasma assisted CVD diamond and assigned as (A, local mode), (B, TA lattice mode), (C, LA lattice mode), and (D, LO lattice mode). Apart from multiphonon sidebands, they reported also an anti-Stokes line labeled E' with 87.6 meV and ascribed it to a local mode. We make, at least partially, a different assignment. Mode B is strong and much narrower than all other sidebands in our spectrum. Also, there is no lattice mode with a high density of states around 65 meV expected to couple to the electronic NP transition. Therefore we ascribe the 64.6-meV line to a local defect mode. The 42-meV mode has low energy and cannot be explained as due to the coupling of a regular lattice mode to the defect. Modes with similar vibration energy around 42 meV have been observed for a variety of optical centers, such as the $N3$ center (2.985 eV), the $H3$ center (2.464 eV), and the $H4$ centers (2.417 eV and 2.53 eV)—which are all associated with nitrogen—but also for

TABLE I. Phonon energies in the 1.681-eV luminescence spectrum and, as an example for comparison, in the $N3$ (2.985-eV) spectrum. Labels A through D refer to the notation of Feng and Schwartz (Ref. 11). (*) The peak at 87.6 meV was seen in Ref. 11 as an anti-Stokes satellite (labeled E') energetically above the NP transition. (**) Very weak feature in the $N3$ spectrum together with a similarly weak peak at ~ 133-meV line shift.

Labels of Ref. 11	Line shift from NP line (meV) 1.681-eV center Present work	1.681-eV center Ref. 11	2.985-eV ($N3$) center Ref. 15	Assignment
A	42	42.0	~ 43	Local mode
B	64.6	64.6		Local mode
	85	(87.6)*	87	
C	125.5	125.3	(125)**	
D	153	153.6	155	LO/LA ?
	166			O^Γ

$GR1$ (1.673 eV) which is ascribed to the neutral vacancy with no impurity involved.[12] This demonstrates that the mode is not specific to the 1.681-eV center and is not an indication of nitrogen being incorporated in the center. Instead, the low phonon energy could arise due to local softening of the crystal around the defect as has been discussed previously in the literature in conjunction with other defects.[13,14] Among the remaining modes with $\hbar\Omega$ = 85, 125.5, and 153 meV, only the 153-meV mode can with some certainty be assigned to LO lattice vibrations coupling with an energy close to their maximum density of states value. In contrast, there is no particular feature around 125.5 meV in the phonon density of states of natural or synthetic bulk crystals. [Here, we refer to the second order Raman spectrum which reflects the density of states and where 125.5 meV (1012 cm^{-1}) corresponds to twice the frequency, 2025 cm^{-1} (Ref. 16)]. However, at this vibration energy, the second order Raman spectrum of microwave CVD films exhibits a pronounced broad peak,[17] and also the one-phonon absorption of such films rendered allowed by disorder effects in the CVD diamond shows a broad peak.[17] We tend to associate the 125.5-meV mode in our spectrum to such a perturbed lattice spectrum. In this context it should be pointed out that the homoepitaxial film used in our work is by no means perfectly crystalline and homogeneous, as discussed later, and in fact could show disorder or local strain effects. As for the 85-meV mode, there is no satisfactory explanation in terms of unperturbed lattice vibrations and their density of states. Modes of 125 meV and 87 meV, close to the present case, are also observed in the comparable case of the $N3$ center,[15] indicating that these modes are not defect specific. Finally, the sharp sideband at $\hbar\Omega$ = 166 meV that we observe is clearly due to the coupling of an O^{Γ} zone center lattice mode in which the two sublattices of diamond locally vibrate around the optical center. There was no indication of this mode in previous PL spectra of CVD diamond including, in particular, the spectrum of the 1.681-eV center by Feng and Schwartz.[11] In our sample, this vibrational satellite line was not always observed and depended on the position of the excited spot on the sample surface.

The inset of Fig. 1 shows the fine structure of the NP line at T = 20 K. The doublet structure [components (b) and (c) at 1.6820 eV and 1.6828 eV, respectively] is fully resolved and exhibits extra components (a) and (d) on its asymmetrically shaped outer wings with photon energies of 1.6817 eV and 1.6830(5) eV, respectively. This quartet is the main mirrorlike fine structure. At least three more weak components occur at 1.681 eV (α), 1.6813 eV (β), and 1.6824(5) eV (γ). Another weak component is positioned at 1.6805 eV (arrow in Fig. 1). The basic doublet structure consisting of the lines (b) and (c) has very recently been reported by Collins *et al.*[10] in a less well resolved spectrum in polycrystalline CVD diamond. The relative intensities of the main components (b) and (c) as a function of temperature are shown in Fig. 2 as an Arrhenius plot. Line (c) is exponentially activated relative to line (b), according to a Boltzmann law $\frac{I(c)}{I(b)} = \text{const} \times \exp(-\Delta E_{th}/k_B T)$. The experimental line intensities were taken as the area under the lines

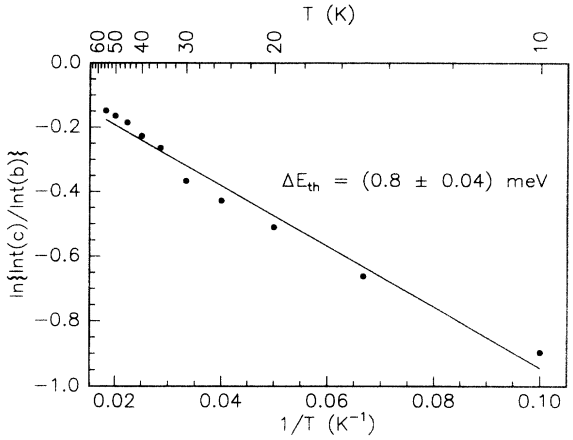

FIG. 2. Arrhenius plot of the intensity ratio of the NP line components (c)–(b) versus reciprocal temperature. The thermal activation energy of the intensity ratio is ΔE_{th} = (0.80 ± 0.04) meV (full line) as obtained from a least squares fit to the data.

after a computer-assisted decomposition of the NP spectrum. A least squares fit to the data in Fig. 2 yields ΔE_{th} = (0.80 ± 0.04) meV. The constant reflects the ratio of the line transition strengths including degeneracies and is ≈ 1. ΔE_{th} is equal to the spectroscopic spacing of the lines (b) and (c), hence the line splitting occurs in the luminescence excited state. This result is equal to the recent finding of Collins *et al.*[10] who report an activation energy of (0.76 ± 0.04) meV.

Our position of the principal NP line is 1.682 eV, 1 meV higher than usually cited in the literature. To have more data on hand on the exact PL line position we measured a variety of samples (all polycrystalline apart from the present homoepitaxial sample). The PL line posi-

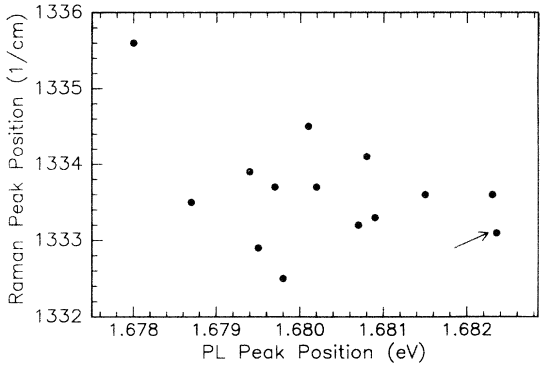

FIG. 3. Positions of Raman (O^{Γ}) peaks at 300 K versus corresponding PL line positions of the 1.681-eV center at 4.2 K in a variety of CVD polycrystalline and homoepitaxial samples. The arrow indicates the homoepitaxial sample mainly investigated in this work. In this case, the spectrum was recorded with wide slits averaging out the NP fine structure for comparison with the other samples. Uncertainty on PL scale is < 0.3 meV (arrowed sample < 0.1 meV), uncertainty on Raman scale is ≈ 0.5 cm^{-1}.

tions were compared to the Raman line positions in the same sample (Fig. 3). There is no simple relation between the PL and Raman line shifts. However, the three highest PL peak positions are associated with the narrowest PL half widths among the sample investigated. Of these three samples, the two polycrystalline films do not show any fine structure splitting. Collins *et al.*[10] who observe the (*b*) and (*c*) line components have their (*b*) line positioned at 1.6815 eV; averaging over their (*b*) and (*c*) components, the transition is close to 1.682 eV. This comparison leads us to conclude that in our homoepitaxial sample we are observing the unstressed position of the optical defect spectrum.

II. EFFECT OF UNAXIAL STRESS

Uniaxial stress was applied to the homoepitaxial film in order to observe line splittings and to obtain information on the underlying defect level scheme. In our particular sample, the film plane is (001), according to the growth on the ⟨001⟩ substrate, and all four side faces of the substrate are also {001} type. Therefore, uniaxial stress **p** could only be applied along one of the ⟨001⟩ directions. Experimentally, we have chosen to apply the stress via movable pistons to two opposite vertical side faces of the substrate. They have an area of 3×0.5 mm^2 each. For this ⟨001⟩ stress direction, measurements were performed up to p= 0.5 GPa at fixed temperatures between 10 K and 15 K in PL and PLE, and at a given stress value p around 0.1 GPa at controlled temperatures from 13 K to 80 K in PL. In the PLE measurements, PL detection was on the 64.6-meV local mode sideband while the exciting laser was tuned to higher energies. Stress dependent data are shown in Fig. 4.

In PL, the components (*a*), (*b*), and (*c*) are split apart by the stress where (*a*) and (*b*) obviously do not thermalize but (*c*) disappears when the spacing from (*a*) and (*b*) increases. In PLE—which is equivalent to an absorption experiment—the components (*b*), (*c*), and (*d*) are split apart by the stress where (*b*) and (*d*) remain strong and (*c*) seems to disappear at larger spacings from (*b*) and (*d*). The component (*a*) very rapidly drops in intensity. The components (*b*) and (*d*) develop a partially resolved doublet structure which we have observed in several independent measurements probably excluding an artifact due to stress inhomogeneities. Combining the PL and PLE data, the external stress splits the four zero-stress components apart and splits the two inner and dominant components (*b*) and (*c*) of the zero-stress spectrum into close doublets. At present we are unable to interpret this close doublet splitting.

The peak splitting pattern is shown in Fig. 5. It is almost symmetric with low shift rates of (*b*) and (*c*), and significantly higher shift rates of (*a*) and (*d*). The spacing of (*a*) and (*b*) is the same as that of (*c*) and (*d*). All splittings are linear in the stress. Eye guidelines are drawn through the data points. Those for the components (*a*) and (*b*) and for (*c*) and (*d*) pairwise intersect at a stress of $p_0 \approx -0.06$ GPa. The inset of Fig. 5 exhibits a four level scheme in which the upper state is split by Δ_{up} and the lower state is split by Δ_{low}. This level scheme is consistent with the splitting pattern and with detailed thermalization measurements which have been performed in PL and PLE and are shown in Fig. 6. In PLE, the intensity ratio of (*d*) to (*b*), $R_{d/b}$, is constant as a function of the spectroscopic spacing Δ_{spect} of the two components. This demonstrates that they initiate from the same lower level. As stated earlier, in PL the intensity ratio $R_{b/a}$ is independent as well of the corresponding spectroscopic spacing $\Delta_{\mathrm{spect}} = \Delta_{\mathrm{low}}$ demonstrating that these components initiate from the same upper level. The remaining intensity ratios in Fig. 6 follow approximately the dependences:

$$\begin{aligned} \text{PLE}: \quad & R_{b/c} \approx 0.4 \times \exp(1.1\Delta_{\mathrm{spect}}/k_BT) \\ & R_{d/c} \approx 0.34 \times \exp(0.8\Delta_{\mathrm{spect}}/k_BT) \\ & R_{b/a} \approx 0.5 \times \exp(2.2\Delta_{\mathrm{spect}}/k_BT) \\ \text{PL}: \quad & R_{b/c} \approx 1 \times \exp(1.8\Delta_{\mathrm{spect}}/k_BT) \end{aligned}$$

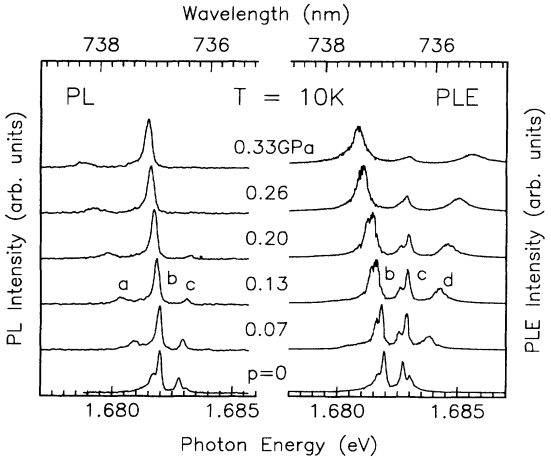

FIG. 4. Left: Splitting of the no-phonon PL spectrum at 10 K under uniaxial stress up to p= 0.33 GPa along ⟨001⟩. Right: Corresponding PLE spectra with light detection on the 64.6-meV local mode satellite of the optical center.

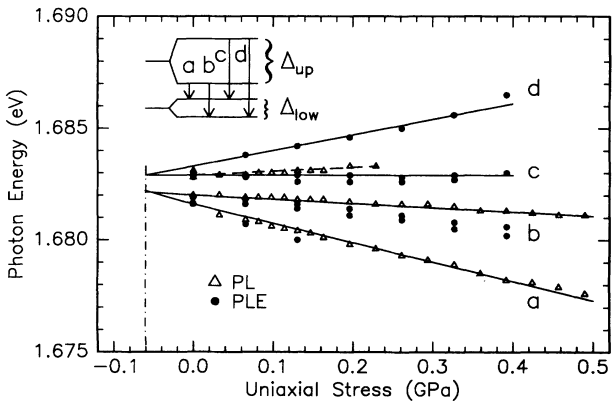

FIG. 5. Splitting pattern for stress **p** ||⟨001⟩ on the basis of PL (triangles) and PLE (dots) measurements. Straight lines are eye guides. The level scheme (inset) is consistent with the splitting data and the thermalization data of Fig. 6.

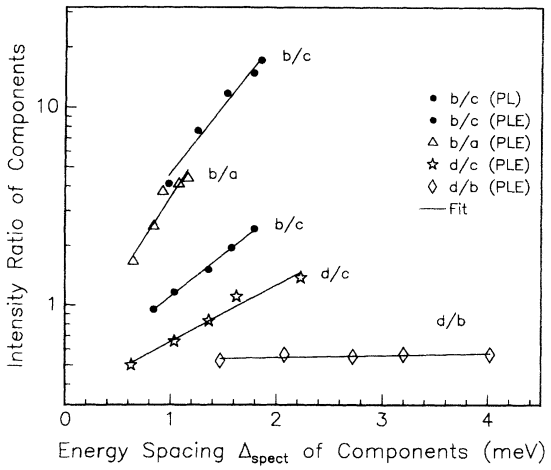

FIG. 6. Thermalization behavior of various line components under stress in PL and PLE measurements at $T = 13$ K.

(Note that in these expressions Δ_{spect} is not a unique parameter but individually corresponds to the two chosen line components.) For $R_{b/c}$ and $R_{d/c}$, Δ_{spect} is equal to the lower level splitting Δ_{low}. Correctly, for PLE the prefactors in the exponentials are close to unity proving thermalization in the initial state. For $R_{b/a}$, the prefactor of 2.2 deviates strongly from 1; however, as shown in Fig. 5, the (a) component is extremely weak in PLE and therefore, the intensity ratio has a large uncertainty giving $R_{b/a}$ little weight in our discussion. The transitions (b) and (c) have different initial and final states, and $\Delta_{spect} = \Delta_{up} - \Delta_{low}$. In the splitting regime where the PL data of Fig. 6 were taken, Δ_{up}/Δ_{low} varies from ≈ 2 to ≈ 1.6 as directly seen in Fig. 5. Taking a middle value of $\Delta_{up}/\Delta_{low} \approx 1.8$, Δ_{spect} is obtained as $\Delta_{spect} \approx 0.44\Delta_{up}$. Hence, the PL intensity ratio varies as $R_{b/c} \approx \exp(0.8\Delta_{up}/k_BT)$ again reasonably close to a thermalization with the full upper level spacing Δ_{up}. Finally, in an independent PL experiment, thermalization of the line components has been investigated as a function of temperature for a constant external stress of slightly below 0.1 GPa. Observed was a spectroscopic spacing of (b)–(c) of $\Delta_{spect} \approx 1$ meV, and Δ_{up}, the spacing from (a) to (c), was ≈ 2.1 meV. For this splitting, the intensity ratio of (c)–(b) follows an exponential law with a thermal activation energy of ≈ 1.7 meV. This is definitely more than Δ_{spect} but close to Δ_{up} lending further support to the level scheme in Fig. 6.

The thermalization features discussed here demonstrate that for all transitions thermalization takes place between the respective initial states, "up" in PL and "low" in PLE. At the same time, the final states do not have to be considered for any thermalization and appear "unoccupied" for each of the transitions. This is evidence, that the 1.681-eV defect luminescence can be described in terms of pure electron ("atomic") transitions and that excitonic or electron-hole recombination does not play a role: In the one-particle picture of an exciton, the electron-hole recombination from the initial exciton state occurs to the "vacuum" state which cannot split under stress; light absorption—equivalent to our PLE measurements—cannot be observed with thermalizing initial substates. In a model of bound electron-to-bound hole recombination, both the upper electron states and the lower hole states in the level scheme of Fig. 5 would be subjected to thermalization. This is in contrast to the experimental findings where only the transition initial states thermalize with no indication of thermalization in the final states. However, exactly these latter features are encountered in atomlike transitions involving only electrons. There are many examples of such transitions in the literature. Prominent cases are transition elements in various III-V-compound semiconductors, such as Fe in GaAs, GaP, or InP.[18,19] Finally, we note that the level scheme suggested in Fig. 5 leads to discrepancies for external stress $p = 0$, where (b) and (c) thermalize approximately with their spectroscopic spacing of 0.8 meV but the level splitting in the upper state from which they originate is ≈ 1.3 meV. At present, this inconsistency remains unresolved and could indicate that at low stress the level scheme is not as simple as discussed. Also, due to the asymmetry of the line shapes the influence of the other components cannot easily be assessed and could be a potential source of error.

The splitting pattern of Fig. 5 explains why the shape of the zero-stress lines in Fig. 1 appears asymmetric with smeared outer wings but steep inner slopes. When there are random values of residual internal strain locally affecting individual centers with shift rates as in Fig. 5, the average broadening effect would lead to soft, washed-out outer wings in the spectrum but the inner wings must remain steep as the underlying shift rates are close to zero. This interpretation implies that our homoepitaxial film is far from being perfectly homogeneous despite the very narrow PL lines which the optical center emits. In fact, exciting luminescence on different spots of the surface was found to change the linewidths of the PL fine structure in Fig. 1 leading to less well resolved components or to the absence of the O^{Γ} vibronic satellite line in the spectrum.

The fact that the splittings (a)–(b) and (b)–(c) become zero at a fictitious negative stress of around $p_0 \approx -0.06$ GPa suggests that there is an internal overpressure on the center, and that the external stress adds linearly to the internal stress. The assumption of overpressure in the center is highly plausible when the constituents of the centers are silicon and nitrogen atoms, and a vacancy. The silicon atom is likely to give rise to an internal overpressure because of its large atomic radius relative to the carbon radius in the diamond lattice. Such internal stress is well documented for two irradiation-induced optical centers in silicon, the 0.79-eV defect[20,21] and the 0.767-eV defect.[22,23] In these centers, the strain arises essentially from a "split interstitial" configuration in which two atoms, carbon and silicon, share a lattice site.

III. TIME-RESOLVED MEASUREMENTS

Finally, we have measured the luminescence decay time of the center in the homoepitaxial film and in a poly-

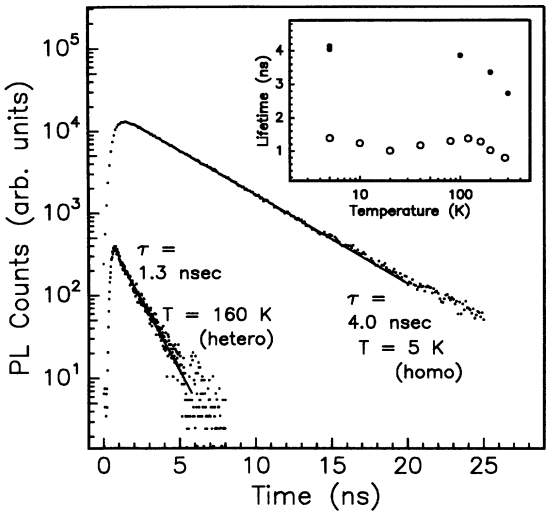

FIG. 7. Intensity decay of the defect luminescence after excitation by a 5-ns laser pulse in the homoepitaxial film at T= 5 K and in a polycrystalline film at T= 160 K. The decay is monoexponential for all temperatures in either sample. The inset shows the decay times as a function of temperature (dots: homoepitaxial film; circles: polycrystalline film).

crystalline diamond layer (Fig. 7). All decay curves are monoexponential over at least one and a half decades. The decay times obtained from these raw data are plotted in the inset as a function of the sample temperature. They vary slightly between 4 ns and 2.7 ns for the homoepitaxial film, and are close to $\tau = 1$ ns and nearly independent of temperature up to $T = 150$ K for the polycrystalline film. The background luminescence decays are much faster with $\tau \leq 500$ ps as was measured at energies above the NP line (725 nm) and at the PL minimum between the NP line and the 42 meV mode (750 nm). The relatively small variation of the decay times with temperature implies that the luminescing, and thermalizing, doublet states have identical or very similar individual lifetimes as otherwise the observed decay times would change according to the thermal repopulation of the two states. We ascribe the significantly shorter PL lifetime in the polycrystalline film either to the existence of competitive recombination channels due to other, nonradiative defects such as dislocation and grain boundaries, or to the presence of high strain in the polycrystalline material. The decay time in the homoepitaxial layer is close to that of the major irradiation-induced defect $GR1$ which has one of its two main luminescence transitions (at 1.673 eV) with $\tau \approx 3$ ns spectrally close to the present 1.681-eV center. Known lifetime data of other point defects are significantly larger, typical examples being the 2.156-eV center with ≈ 29 ns, the 2.463-eV center ($H3$) with 16.7 ns, and the 2.985-eV center ($N3$) with 40 ns.[24]

IV. SUMMARY

In conclusion, we have observed the 1.681-eV defect line in a homoepitaxially grown diamond film with the very narrow linewidth of 0.2 meV and with an energy of 1.682 eV for the main transition. This spectrum reveals a completely resolved doublet structure and at least five additional, partially resolved components. The narrow linewidth was associated with the relatively small residual strain in the homoepitaxial layer as compared to polycrystalline layers. A small residual strain in the homoepitaxial film was concluded from the typical asymmetric doublet line shapes. The stress-induced splitting of the lines in the PL and PLE spectra was explained with a level scheme where both the upper and lower states in the main radiative transition are split into doublets, and thermalization occurs within the initial state of each transition, which is the upper state for PL and the lower state for PLE (absorption). This level scheme suggests a pure electron description of the transition, with no participation of holes or excitons. The optical transition is short lived exhibiting a decay time of between ≈ 1 ns and 4 ns similar to that of the irradiation-induced $GR1$ defect (neutral single-atom vacancy) at the close-by transition energy of 1.673 eV.

ACKNOWLEDGMENTS

Essential support of this work by the gift of various samples comes from O. Weis of the Abteilung Festkörperphysik, University of Ulm. Similarly, B. Lux and R. Haubner of the Institut für chemische Technologie anorganischer Stoffe, Technical University of Vienna, Austria, have contributed a variety of polycrystalline CVD and hot-filament films. We are also grateful to E. Blank of the Département des Materiaux, Ecole Polytechnique Fédérale, Lausanne, Switzerland, for providing two heteroepitaxial CVD samples. J. Gerster and W. Limmer of the Abteilung Halbleiterphysik at the University of Ulm have kindly performed the Raman measurements. One of the authors (P. M.) is grateful to A. Hangleiter and T. Forner of the same institute for their support of the time-resolved measurements. The authors gratefully acknowledge financial support of the present work by the Deutsche Forschungsgemeinschaft (Project No. Sa 520/1-1 and /2-1) carried out under the auspices of the trinational "D-A-CH" cooperation of Germany, Austria, and Switzerland on the "Synthesis of Superhard Materials."

[1] V. S. Vavilov, A. A. Gippius, A. M. Zaitsev, B. V. Derjaguin, B. V. Spitsyn, and A. E. Aleksenko, Fiz. Tekh. Poluprovodn. **14**, 1811 (1980) [Sov. Phys. Semicond. **14**, 1078 (1981)].

[2] L. H. Robins, L. P. Cork, E. N. Farabaugh, and A. Feldman, Phys. Rev. B **39**, 13 367 (1989).

[3] J. A. Freitas, J. E. Butler, and U. Strom, J. Mater. Res. **5**, 2502 (1990).

[4] T. A. Perry and C. P. Beetz, Proc. SPIE **1005**, 152 (1990).
[5] L. S. Plano and K. V. Ravi, Proc. SPIE **1005**, 176 (1990).
[6] Y. Yokota, H. Kawarada, and A. Hiraki, in *Diamond, Boron Nitride, Silicon Carbide and Related Wide Bandgap Semiconductors*, edited by J. T. Glass, R. F. Messier, and N. Fujimori, MRS Symposia Proceedings No. 162 (Materials Research Society, Pittsburgh, 1990), p. 231.
[7] A. T. Collins, M. Kamo, and Y. Sato, J. Mater. Res. **5**, 2507 (1990).
[8] J. Ruan, W. J. Choyke, and W. D. Partelow, Appl. Phys. Lett. **58**, 295 (1991).
[9] A. M. Zaitsev, V. S. Vavilov, and A. A. Gippius, Sov. Phys. Lebedev Inst. Rep. **10**, 15 (1981)
[10] A. T. Collins, L. Allers, C. J. H. Wort, and G. A. Scarsbrook, Diamond Relat. Mater. **3**, 932 (1994).
[11] T. Feng and B. D. Schwartz, J. Appl. Phys. **73**, 1315 (1993).
[12] P. K. Bachmann and D. U. Wiechert, Diamond Relat. Mater. **1**, 422 (1992).
[13] J. Walker, Rep. Prog. Phys. **43**, 108 (1979).
[14] F. P. Larkins and A. M. Stoneham, J. Phys. C **4**, 143 (1971).
[15] A. T. Collins, Physica B **185**, 284 (1993).
[16] S. A. Solin and A. K. Ramdas, Phys. Rev. B **1**, 1687 (1970).
[17] C. Klein, T. Hartnett, R. Miller, and C. Robinson, in *Diamond Materials*, Proceedings of the 2nd International Symposia, edited by A. J. Purdes *et al.* (The Electrochemical Society, Pennington, New Jersey, 1991), p. 435.
[18] W. H. Koschel and U. Kaufmann, Solid State Commun. **21**, 1069 (1977).
[19] G. Rückert, K. Pressel, A. Dörnen, K. Thonke, and W. Ulrici, Phys. Rev. B **46**, 13 207 (1992).
[20] K. Thonke, A. Hangleiter, J. Wagner, and R. Sauer, J. Phys. C **18**, L795 (1985).
[21] J. M. Trombetta and G. D. Watkins, Appl. Phys. Lett. **51**, 1103 (1987).
[22] J. Wagner, A. Dörnen, and R. Sauer, Phys. Rev. B **31**, 5561 (1985).
[23] W. Kürner, R. Sauer, A. Dörnen, and K. Thonke, Phys. Rev. B **39**, 13 327 (1989).
[24] G. Davies, in *The Properties of Diamond*, edited by J. E. Field (Academic Press, London, 1979), p. 165.